

Article

Parameters Optimization and Test of an Arc-Shaped Nail-Tooth Roller-Type Recovery Machine for Sowing Layer Residual Film

Zhiyuan Zhang^{1,2,3} , Jingbin Li^{1,2,3,*}, Xianfei Wang^{1,2,3}, Yongman Zhao^{1,2,3}, Shuaikang Xue^{1,2,3}
and Zipeng Su^{1,2,3}

¹ College of Mechanical and Electrical Engineering, Shihezi University, Shihezi 832003, China; zhangzy@stu.shzu.edu.cn (Z.Z.); wangxf@shzu.edu.cn (X.W.); zhrym@shzu.edu.cn (Y.Z.); 20192009026@stu.shzu.edu.cn (S.X.); szp@stu.shzu.edu.cn (Z.S.)

² Xinjiang Production and Construction Corps Key Laboratory of Modern Agricultural Machinery, Shihezi 832003, China

³ Industrial Technology Research Institute of Xinjiang Production and Construction Corps, Shihezi 832003, China

* Correspondence: lijingbin@shzu.edu.cn

Abstract: The aim of this paper is to optimize the working parameters of the arc-shaped nail-tooth roller-type recovery machine for sowing layer residual film. Firstly, the tooth roller device of the residual film recovery machine is designed, and the main working parameters affecting the operation of the machine and the value range of each parameter are determined through the analysis of the operation process. Secondly, virtual simulation technology is used to establish a virtual simulation model of the interaction process between the tooth roller device and soil. At the same time, taking the soil-hilling quantity as the index, we build a quadratic regression mathematical model with three factors—the forward speed, rotation speed, and working depth—using the Box–Behnken method. Consequently, the analysis of the simulation results show that the order of the most significant factors is working depth, rotation speed, and forward speed. The optimal combination of working parameters are as follows: a forward speed of 4.5 km/h, a rotation speed of 43.2 r/min, and a working depth of 100.0 mm. Meanwhile, the predicted value of the soil-hilling quantity is 23.1 kg. Finally, we carried out field tests using the optimal combination parameters; the results show that the normal residual film collection rate is 66.8%, the soil-hilling quantity is 24.2 kg, and the relative error between the test value and the predicted value is 4.8%. This indicates that the devised DEM simulation model can be used to predict the operational performance of the tooth roller device in the working process. This study provides a reference that can be used in the planning and boundary enhancement of agricultural machinery and equipment.

Keywords: residual film recovery machine; DEM; virtual simulation; parameter optimization; agricultural machinery



Citation: Zhang, Z.; Li, J.; Wang, X.; Zhao, Y.; Xue, S.; Su, Z. Parameters Optimization and Test of an Arc-Shaped Nail-Tooth Roller-Type Recovery Machine for Sowing Layer Residual Film. *Agriculture* **2022**, *12*, 660. <https://doi.org/10.3390/agriculture12050660>

Academic Editors: Mustafa Ucgul and Chung-Liang Chang

Received: 5 April 2022

Accepted: 30 April 2022

Published: 3 May 2022

Publisher's Note: MDPI stays neutral with regard to jurisdictional claims in published maps and institutional affiliations.



Copyright: © 2022 by the authors. Licensee MDPI, Basel, Switzerland. This article is an open access article distributed under the terms and conditions of the Creative Commons Attribution (CC BY) license (<https://creativecommons.org/licenses/by/4.0/>).

1. Introduction

Cotton planting has embraced the established model for film laying and tube laying in Xinjiang, which has reached 100%. In the meantime, the recovery rate of farmland residual film is just 60%, causing a significant amount of residual film to remain in the field, causing genuine white contamination of farmland; this has turned into an unmistakable issue that limits the green advancement of agriculture [1–3]. Mechanized residual film recuperation has developed into an unavoidable pattern in the treatment of residual film contamination [4,5]. In light of the radial plate arc-shaped nail-tooth roller structure, an arc-shaped formed nail-tooth roller-type planting layer residual film recovery machine (hereafter alluded to as the residual film recovery machine) was designed by our group. Field tests have shown that the average recovery rate of the residual film recovery machine is 67%, which can effectively recover residual film from the seeding layer. Nonetheless, the unmatched and unreasonable operation

parameters of the residual film recovery machine have led to the phenomenon of hilling, subsequently resulting in the poor operational effect of the machine [6]. Therefore, the identification of sensible working parameters is important to improve the working efficiency of the residual film recovery machine.

With the widespread application of computer technology in agricultural production, the discrete element method (DEM) is also widely used in the simulation of the working parts of agricultural machinery, such as the process simulation of seeders and subsoilers, and the results can provide a reference for field tests [7]. Zhang [8] and Jiang et al. [9] conducted a simulation test study on the operating performance of the rotating drum device and spiral impurity cleaning device of the residual film recovery machine using DEM, and verified the reliability of the DEM approach combined with field tests. Wang [10], Tong [11], and Hang et al. [12] used DEM to study the influence of a subsoiler on soil tillage force and disturbance characteristics during operation. Dai et al. [13] concentrated on the working presentation of a crosswise belt-type whole plastic film-ridging residual corn seeder on double ridges by combining DEM simulation technology with field experiments, which further verified the superiority of the DEM. Hence, the combination of simulation technology and DEM has commonly been applied in the exploration of the cooperation law between the soil and soil contact of agricultural machinery, and has accomplished great outcomes. Compared with the traditional method of depending on an indoor soil bin test bench or genuine field test to optimize the operating parameters, the virtual simulation test using the DEM can not only shorten the test cycle and decrease the research and development work costs, but can also naturally and precisely control and measure the physical quantities of the machine, such as operation speed, operation depth, load, and soil resistance. Hence, the DEM is frequently utilized in the design, performance testing, and product optimization of agricultural machinery and equipment.

In view of the past research, this paper principally concentrates on the influence of various working parameters on the quality of soil hilling when the residual film recovery machine works using theoretical analysis, DEM simulation, and field testing. We obtain the scope of the key variables that influence the efficiency of the tooth roller device's activity by theoretical analysis. Moreover, we use the DEM to set up the simulation model between the soil and the tooth roller device. In addition, we find the optimum working parameters of the tooth roller device through response surface methodology, and validate the accuracy of the simulation results using the indoor soil trough test. This review can give significant hypothetical premise and specialized help for the design and parameter optimization of the key components of agricultural machinery equipment such as the residual film recovery machine.

2. Materials and Methods

2.1. Structure of Residual Film Recovery Machine

The residual film recovery machine fundamentally comprises the traction unit, the rack, the drive system, the tooth roller device, the film stripping unit, the depth-limiting wheel, and the film collection unit, as displayed in Figure 1. The proposed residual film recovery machine was trailed by a working tractor. The power take-off (PTO) shaft of the work tractor gives power to the drive system, and at that point, the drive framework distributes the power to the tooth roller device and the film-stripping unit to pick and strip residual films effectively.

2.2. Design and Analysis of Tooth Roller Device

2.2.1. Design of Tooth Roller Device

The tooth roller device is the critical part of the residual film recovery machine, which mostly comprises the arc-shaped nail-tooth, base, flange, shaft head, central tube, and radial plate, as shown in Figure 2. The compelling working width is 1600 mm, the most extreme rotating diameter is 950 mm, and the distance between the two spiral plates is

236 mm. The bases are uniformly distributed in the peripheral direction of the tooth roller device. There are 12 or 13 arc-shaped nail-teeth on each row of holders. The distance between two adjacent teeth is 100 mm, and the circumferential arc-shaped nail-teeth are arranged in staggered mode.

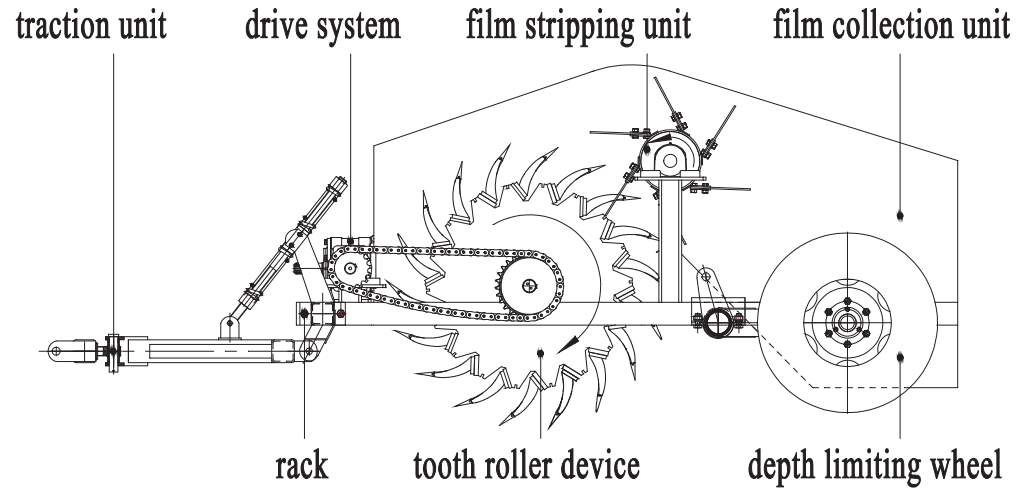


Figure 1. Structure of the residual film recovery machine.

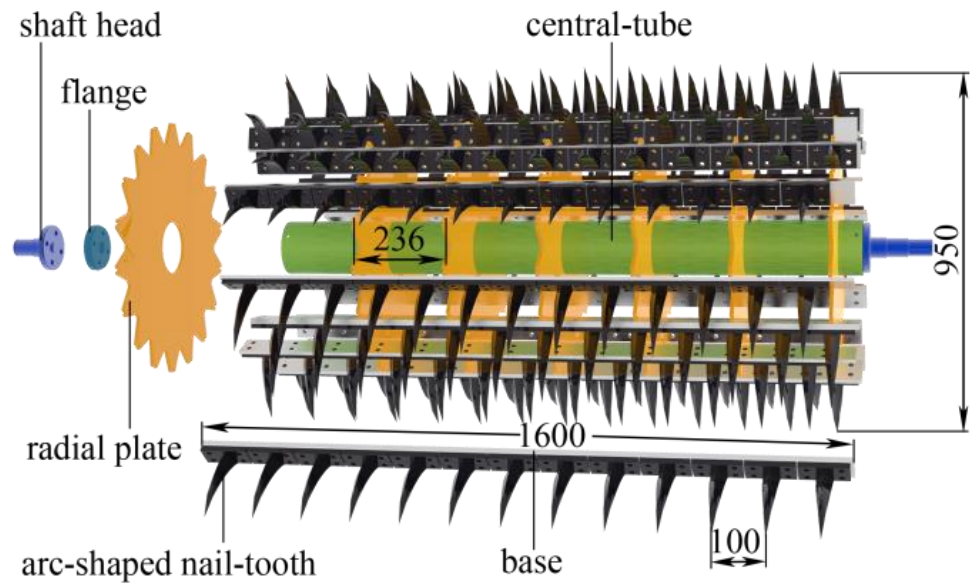


Figure 2. Structure diagram of the tooth roller device.

2.2.2. Analysis of Film-Picking Operation of Arc-Shaped Nail-Teeth

To finish the picking activity, the nail-teeth pierce through the residual film with the tooth tip when the machine is working. Meanwhile, the residual film is moved along with the arc-shaped nail-teeth to isolate it from the soil. Therefore, the residual film in the soil was taken as the research object for force analysis, and the rectangular coordinate system $o-xy$ established with the o point, as shown in Figure 3.

The forces can be decomposed along the x -axis and y -axis, as follows:

$$\begin{cases} f + F_N = F_Z + F_L \cdot \cos \theta \\ F_L \cdot \sin \theta = mg \cdot \sin \delta + f_L \\ F_N = Mg \cdot \cos \delta \\ F_L = (M + m) \cdot v^2 / R \\ v = 2\pi Rn \end{cases} \quad (1)$$

where mg is simply the gravity of the residual film, N; Mg is the gravity of soil on the film, N; F_Z is the force on the residual film when the arc-shaped nail-tooth is tied, N; F_N is the pressure of the soil on the residual film while it is attached with the curve-formed nail-tooth, N; F_L is the force on the residual film when the tooth roller device rotates, N; f is the frictional resistance of the residual film to the arc-shaped nail-tooth during operation, N; f_L is the frictional resistance of soil to residual film during operation, N; θ and δ are the angles, rad; and n is the rotation speed, r/min.

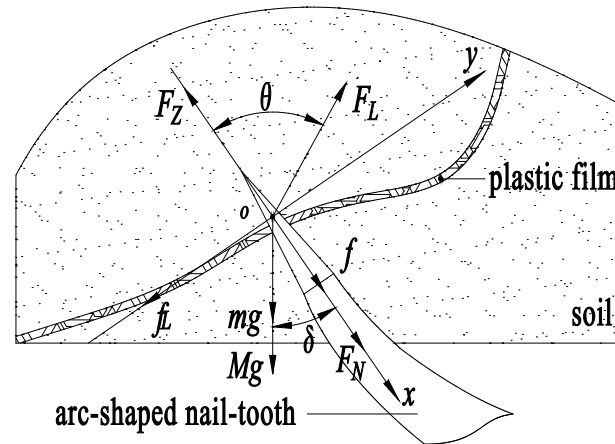


Figure 3. Schematic diagram of residual film force analysis during film-picking operation.

According to the empirical formula [14], the work used by the tooth roller device to rotate once is:

$$\begin{cases} Q = \frac{2\pi M_0}{zShb} + \frac{0.1F}{hb} \\ M_0 = F_Z \cdot R \end{cases} \quad (2)$$

where Q is the work, J; z is the number of arc-shaped nail-teeth, pcs; S is the penetration pitch between adjacent arc-shaped nail-teeth, mm; h is the working depth, mm; b is the width of the arc-shaped nail-tooth, mm; F is the traction force of the machine, N; M_0 is the torque, N m; and R is the radius of the tooth roller device, mm.

Since the mulching film gravity mg is very tiny, it can be ignored. In combination with (1) and (2):

$$Q = \frac{2\pi [4\pi^2 R^2 n^2 M \cdot (\sin \theta + \cos \theta) - (Mg \cdot \cos \delta - f - f_L) \cdot R] + 0.1zSF}{zShb} \quad (3)$$

From Equation (3), we can see that when the structural parameters of the tooth roller device are fixed, the work used in the operation is related to the working parameters of the tooth roller speed, the quality of the soil on the film, and the working depth.

2.2.3. Determination of Tooth Roller Device Operation Parameters

If the rotation speed goes much faster when the tooth roller device is working, the disturbed soil is thrown forward, and the residual film on the tooth roller device moves with the soil. This is not helpful for the film-picking activity of the device. In contrast, if the rotation speed goes much slower, the soil generated by the disturbance will cause soil hilling in front of the residual film recovery machine, thus reducing the operating efficiency of the device and increasing energy consumption during the machine's activity. However, in our field test of the arc-shaped nail-tooth roller-type sowing layer residual film recovery machine, we found that an appropriate amount of soil hilling was conducive to the film-picking activity of the model. Henceforth, it was of extraordinary importance to look for sensible operation parameters to further develop the efficiency of the tooth roller device's operation.

The motion of the tooth roller device during its operation is compound motion, wherein the rotational motion around the center axis of the flanged drum is relative, and

the motion along with the tractor is implicated motion. Thus, the motion track of the arc gear binding vertex D during the rotation of the tooth roller device is the trochoid, as shown in Figure 4.

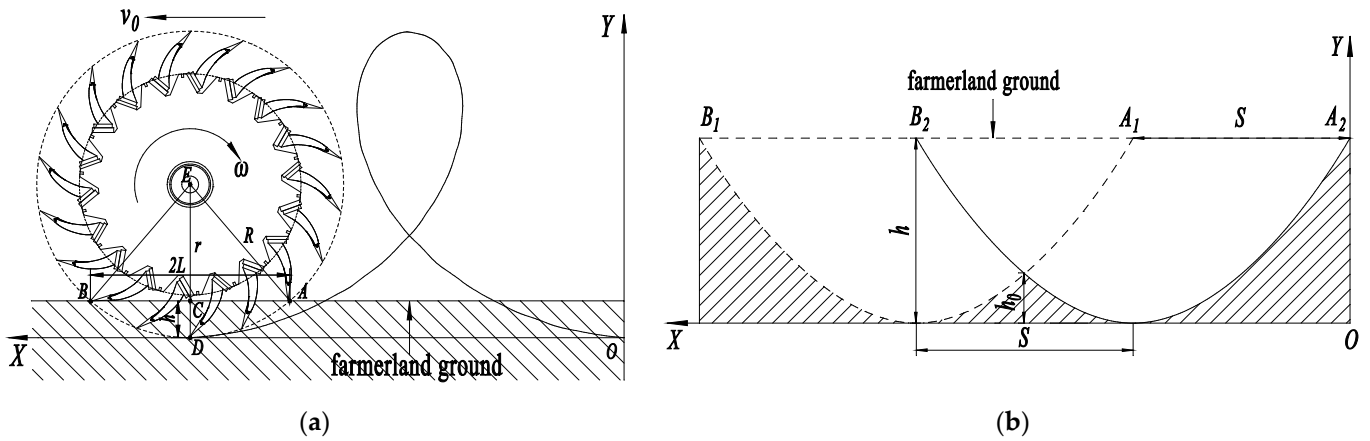


Figure 4. Motion analysis of the tooth roller device. (a) Movement trail of the arc-shaped nail-tooth; (b) analysis of continuous work process.

In Figure 4a, the trochoid is the motion trajectory OD of the tooth tip D on the tooth roller device. The rectangular coordinate system O - XY is established with the point O when tooth tip D enters the deepest soil as the origin, the straight line OD as the X -axis, and the straight line opposite to OD going through O as the Y -axis. Then, at that point, the trajectory equation of the arc-shaped nail-tooth tip motion is:

$$\begin{cases} x = v_0 \cdot t + R \cdot \sin(\omega t) \\ y = R - R \cdot \cos(\omega t) \\ \lambda = v/v_0 > 1 \end{cases} \quad (4)$$

where R is the maximum rotation radius of the tooth roller device, mm; ω is the angular velocity of rotation, rad/s; v is the moving speed of the tooth tip D , m/s; v_0 is the forward speed of the tractor, m/s; t is the movement time, s; and λ is the speed ratio.

The field test results of the residual film recovery machine in the early stage showed that when the working velocity was $v_0 = 4\text{--}6$ km/h, the residual film recovery machine performed well and could complete the recovery of the residual film. Therefore, the forward speed of the machine is settled as $v_0 = 4\text{--}6$ km/h, $\lambda = 3\text{--}10$, and we could obtain the rotational angular velocity of the gear roller device by taking them into Equation (4): $\omega = 2.14\text{--}14.43$ rad/s. According to the relationship between the angular velocity of the circular motion and the velocity when the rigid body rotates, the rotation speed of the tooth roller device can be obtained as $n = 20.43\text{--}137.80$ r/min.

The tooth roller device ought to guarantee that the residual film inside the extent of the sowing layer has been obtained, and guarantee that the residual film in the sowing layer was not missed during operation. Thus, the number of teeth embedded into the soil was one of the key factors that influenced operational efficiency. In addition, related studies show that in order to guarantee that the residual film in the soil does not leak when picked up, at least one arc-shaped nail-tooth remained in the soil when the first tooth was unearthed [1].

In Figure 4a, AE is the maximum rotation radius of the nail-tooth roller on the tooth tip D , $AE = R$, mm; EC is the radius of the tooth roller device, $EC = r$, mm; AB is the distance between the relative track of the tooth tip D relative to the rotation center E of the tooth roller device and the ground, and $AC = BC = L$, mm; and CD is the operating depth, $CD = h$, mm. Then, in $Rt\Delta ACE$, there is:

$$\begin{cases} R^2 = L^2 + r^2 \\ r = R - h \end{cases} \quad (5)$$

In Figure 4b, when the circumferential adjacent arc-shaped nail-teeth pierce through the films, there will be a protruding part in the soil. The protruding height h_0 is the distance from the joint of the trajectories of the arc-shaped nail-teeth to the maximum penetration depth of the nail-teeth. The cotton-sowing depth in Xinjiang is 25–35 mm, so the effective working depth of an arc-shaped nail-tooth is 140 mm. Then:

$$35 \text{ mm} \leq h - h_0 \leq 140 \text{ mm} \quad (6)$$

The area of residual plastic film in the Xinjiang cotton field is mostly 400–2500 mm² [15, 16]. To simplify the calculation model, it can be considered that the shape of the residual film is square, and its side length is $l = 20\text{--}50$ mm. Then, the numbers of teeth N in the circumferential soil acquired by associating Equations (5) and (6) is:

$$N_{\min} = L_{\min}/l_{\max} = 3.57 \quad (7)$$

That is, the number of teeth in the circumferential soil $N_{\min} = 3$. When the circumferential adjacent nail-teeth successively penetrate the soil at time t , the distance of the device in the forward direction is the penetrating pitch S :

$$S = v_0 \cdot t = L/N \quad (8)$$

According to the structure of the tooth roller device, the interval time of the successively penetrated circumferential adjacent arc-shaped nail teeth is:

$$t = \frac{2\pi}{z\omega} \quad (9)$$

where z is the number of rows of installed circumferential arc-shaped nail-teeth, row.

As indicated by Equations (4)–(9) above, it tends to be acquired that $z = 5.9\text{--}19.8$, working depth $h = 43.8\text{--}140.0$ mm. In this paper, according to the geometric characteristics of residual film in farmland, $z = 18$ was chosen to improve the picking efficiency of the residual film recovery machine and increase the number of wrapping films with arc-shaped nail-teeth.

2.3. DEM Simulation Model Establishment

2.3.1. Simulation Modeling

The particle contact model is a fundamental basis for the accuracy of the calculation results of the simulation analysis model. To accurately simulate the interaction behavior between the soil and tools in the actual production process, the soil particle radius was set to 2.5 mm and the soil particle contact model selected was the Hertz–Mindlin with the JKR model by referring to references [8,9,17,18]. To speed up the simulation calculation, one-third of the total length of the tooth roller device was selected as the geometry simulation model; the 3D modeling was carried out with SolidWorks 2016 software (Dassault Systèmes S.E., Massachusetts, Concord, MA, USA) in the proportion 1:1, and was saved in the format of “-.step” and imported into the EDEM 2020 software (DEM Solutions Ltd., Edinburgh, Scotland, UK). As indicated by the underlying size of the geometry simulation model, the size of the particle factory was established as $L \times W \times H = (4000 \times 700 \times 250)$ mm. The simulation model of the soil particles and geometry are displayed in Figure 5.

2.3.2. Simulation Parameter Settings

The simulation fixed time step was set to 6.12×10^{-5} s, the simulation time was set to 14.00 s, the simulation data storage interval was set to 0.05 s, and the mesh cell size of the geometry simulation model was set to 3.00 mm. According to the requirements of the simulation parameters in the virtual simulation test as well as the literature [8,9,19–22], the intrinsic parameters (density, Poisson’s ratio, and shear modulus) and contact parameters

(recovery coefficient, static friction coefficient, and dynamic friction coefficient) of the soil and geometry in this study were determined, as shown in Table 1.

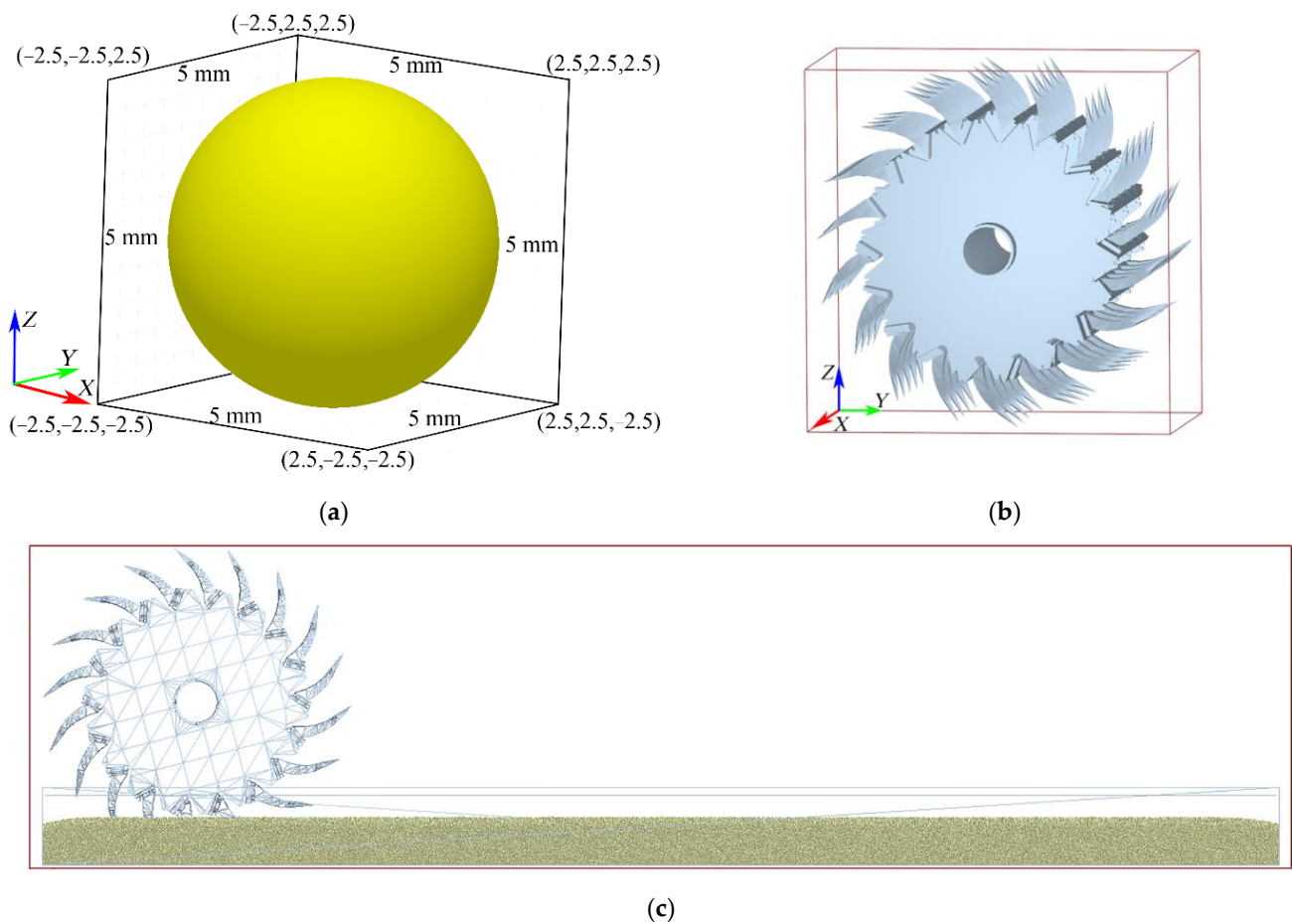


Figure 5. Particle and geometric simulation model. (a) Particle model of the soil; (b) geometric model of the tooth roller device; (c) simulation model of the EDEM.

Table 1. Simulation parameter settings of soil particles and geometry.

Item	Parameter	Value
Soil particles	Poisson's ratio	0.40
	Shear modulus/MPa	1.09×10^6
	Density/($\text{kg}\cdot\text{m}^{-3}$)	1400.00
Arc-shaped nail-tooth	Poisson's ratio	0.30
	Shear modulus/MPa	7.90×10^{10}
	Density/($\text{kg}\cdot\text{m}^{-3}$)	7850.00
Particle—Particle	Recovery coefficient	0.20
	Static friction coefficient	0.40
	Dynamic friction coefficient	0.30
Particle—Arc-shaped nail-tooth	Recovery coefficient	0.30
	Static friction coefficient	0.40
	Dynamic friction coefficient	0.10

2.3.3. Design of Simulation Test

In the field experiments, the research group found that an appropriate soil-hilling phenomenon was conducive to the film-picking activity of the drum device. Therefore, the quality of soil accumulated on the ground (hereafter referred to as the soil-hilling

quantity) was determined as the test response index. In addition, according to the analysis results in 2.2.2 and 2.2.3, the main operating parameters that affect the operation of the device were selected as the forward speed of the machine, the rotation speed of the nail-tooth roller, and the working depth, and the value range of each parameter was 4–6 km/h, 20.43–137.80 r/min, and 43.8–140.0 mm, respectively. Therefore, we used the forward speed of the machine v_0 , the rotation speed of the nail-tooth roller n , and the working depth h as the simulation test factors, and the quality of the soil hilling Y as the testing indicators. The Box–Behnken test module method of Design-Expert V8.0.6.1 software (Stat-Ease Inc., Minneapolis, MN, USA) was used to design a central combined test with three factors and three levels, as shown in Table 2.

Table 2. Horizontal coding table of experimental factors.

Levels	Factors		
	$v_0/\text{km}\cdot\text{h}^{-1}$	$n/\text{r}\cdot\text{min}^{-1}$	h/mm
Upper level (1)	6.00	140.00 (137.80)	140.00
Zero level (0)	5.00	80.00	90.00
Lower level (−1)	4.00	20.00 (20.43)	40.00 (43.75)

3. Results and Discussion

3.1. Regression Analysis of Test Results

The Box–Behnken central combination tests comprised 17 groups, including 12 groups of analysis factors and 5 groups of zero-point estimation error tests. The analysis factor tests were repeated three times in each group, and the results were calculated as an arithmetic average. The experimental design and results are shown in Table 3.

Table 3. Experimental design and results.

No.	Factors and Levels			Response Index
	$A/\text{km}\cdot\text{h}^{-1}$	$B/\text{r}\cdot\text{min}^{-1}$	C/mm	Y/kg
1	4.00	20.00	90.00	8.14
2	6.00	20.00	90.00	22.89
3	4.00	140.00	90.00	16.21
4	6.00	140.00	90.00	27.11
5	4.00	80.00	40.00	6.84
6	6.00	80.00	40.00	16.46
7	4.00	80.00	140.00	34.37
8	6.00	80.00	140.00	49.02
9	5.00	20.00	40.00	3.26
10	5.00	140.00	40.00	10.51
11	5.00	20.00	140.00	36.48
12	5.00	140.00	140.00	39.37
13	5.00	80.00	90.00	25.99
14	5.00	80.00	90.00	25.87
15	5.00	80.00	90.00	26.64
16	5.00	80.00	90.00	25.63
17	5.00	80.00	90.00	26.87

Note: A is the forward speed of machinery, km/h; B is the rotating speed of nail-tooth roller, r/min; C is working depth, N; Y is the soil-hilling quantity, kg.

We conducted multiple linear quadratic regression analyses on the simulation test results in Table 3 using the Design-Expert V8.0.6.1 software. The results are shown in Table 4.

The value of the model for the soil-hilling quality Y was $p < 0.0001$, the value of the lack-of-fit term $p > 0.1$, the second-order response model determination coefficient $R^2 = 99.90\%$, the correction determination coefficient $R^2_{adj} = 99.77\%$, and the prediction determination coefficient $R^2_{pred} = 99.07\%$. This showed that the regression model is extremely significant, and could predict and optimize the soil-hilling quality Y of the tooth roller device under different working parameters. According to the regression analysis of the variance of the

results, multiple regression fitting analysis was conducted on the test results. Equation (10) is the mathematical regression model of the true value of each influencing factor on the response value.

Table 4. Variance analysis of regression models.

Index	Difference Source	Sum of Squares	Degree of Freedom	Mean Square	F-Value	p-Value
Quantity of soil hilling/kg	Model	2432.62	9	270.29	778.21	<0.0001
	A	311.50	1	311.50	896.86	<0.0001
	B	62.89	1	62.89	181.06	<0.0001
	C	1865.69	1	1865.69	5371.59	<0.0001
	AB	3.71	1	3.71	10.67	0.0137
	AC	6.33	1	6.33	18.21	0.0037
	BC	4.75	1	4.75	13.68	0.0077
	A ²	11.78	1	11.78	33.91	0.0006
	B ²	148.56	1	148.56	427.73	<0.0001
	C ²	19.37	1	19.37	55.78	0.0001
	Residual	2.43	7	0.35		
	Lake of Fit	1.31	3	0.44	1.56	0.3304
Pure Error	1.12	4	0.28			

$$R^2 = 99.90\%; R^2_{adj} = 99.77\%; C.V. = 0.41\%; R^2_{pred} = 99.07\%$$

Note: $p < 0.05$ (highly significant); $0.05 < p < 0.1$ (significant); $p > 0.1$ (not significant).

$$Y = -79.36 + 21.98 \cdot A + 0.42 \cdot B + 0.05 \cdot C - 0.02 \cdot AB + 0.03 \cdot AC - 3.63 \times 10^{-4} \cdot BC - 1.67 \cdot A^2 - 1.65 \times 10^{-3} \cdot B^2 + 8.58 \times 10^{-4} \cdot C^2 \tag{10}$$

3.2. Analysis of Interaction between Experimental Factors and Indicators

3.2.1. Influence of Forward Speed and Rotation Speed on Soil-Hilling Quantity

As shown in Figure 6, when the working depth h is at the level of 0 ($h = 90.0$ mm), the interaction between the machine forward speed v_0 and the rotation speed n can have an important impact on the soil-hilling quantity Y . As the forward speed v_0 of the machine tool increases, the soil-hilling quantity Y increases and its change becomes slower. Meanwhile, the rotation speed n increases, the soil-hilling quantity Y increases at first, and then decreases, and its change tends to be faster. This indicates that the influence of rotation speed n on the soil-hilling quantity Y is more significant than the influence of the forward speed of the machine v_0 .

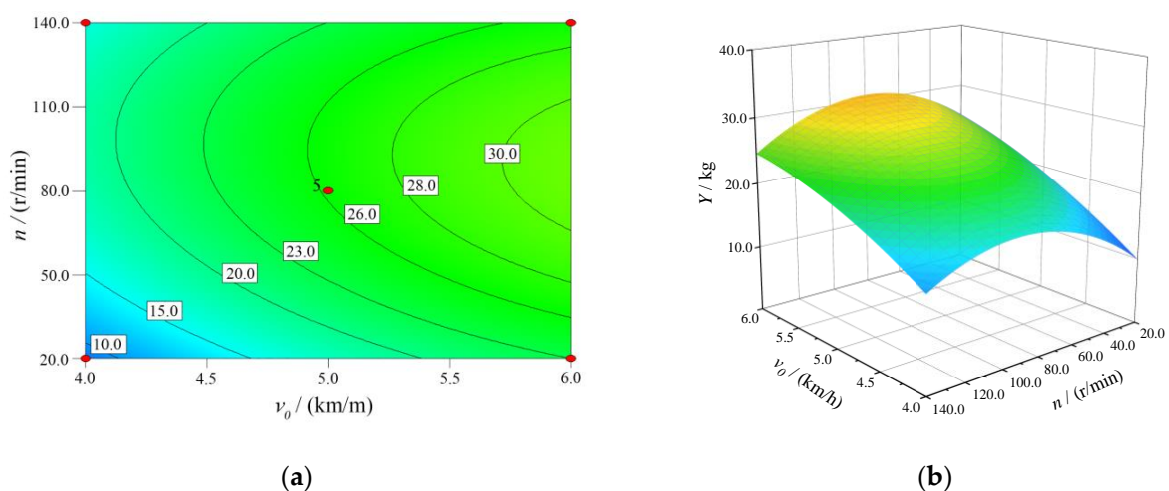


Figure 6. Influence of the forward speed and rotation speed on the soil-hilling quantity. (a) Contour map; (b) response surface diagram.

3.2.2. Influence of Forward Speed and Working Depth on Soil-Hilling Quantity

As shown in Figure 7, when the rotation speed n is at the level of 0 ($n = 80.0$ r/min), the interaction between the operating speed v_0 and the working depth h affects the soil-hilling quantity Y . According to the figure, the soil-hilling quantity Y increases and its variation range slows when the forward speed v_0 increases. As the working depth h increases, the soil-hilling quantity Y increases correspondingly, and its variation range becomes faster. This shows that the effect of working depth h on the soil-hilling quantity Y is more significant than that of the working speed v_0 .

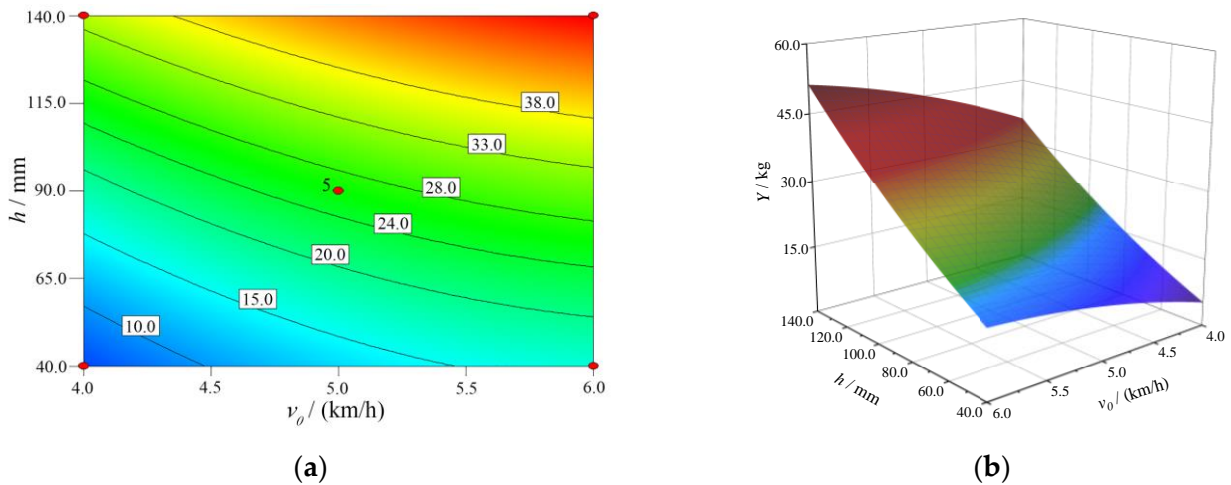


Figure 7. Influence of the forward speed and working depth on the soil-hilling quantity. (a) Contour map; (b) response surface diagram.

3.2.3. Influence of Rotation Speed and Working Depth on Soil-Hilling Quantity

As shown in Figure 8, the forward speed of the machine v_0 is at the level of 0 ($v_0 = 5.0$ km/h), the interaction between rotation speed n and working depth h also affects the soil-hilling quantity Y . It can be seen that when the working depth h increases, the soil-hilling quantity Y increases rapidly and its change range becomes faster; when the rotation speed n increases, the soil-hilling quantity Y begins increasing and then decreases with a slower change range. This shows that the impact of the working depth h on the soil-hilling quantity Y is more significant than that of the rotation speed n .

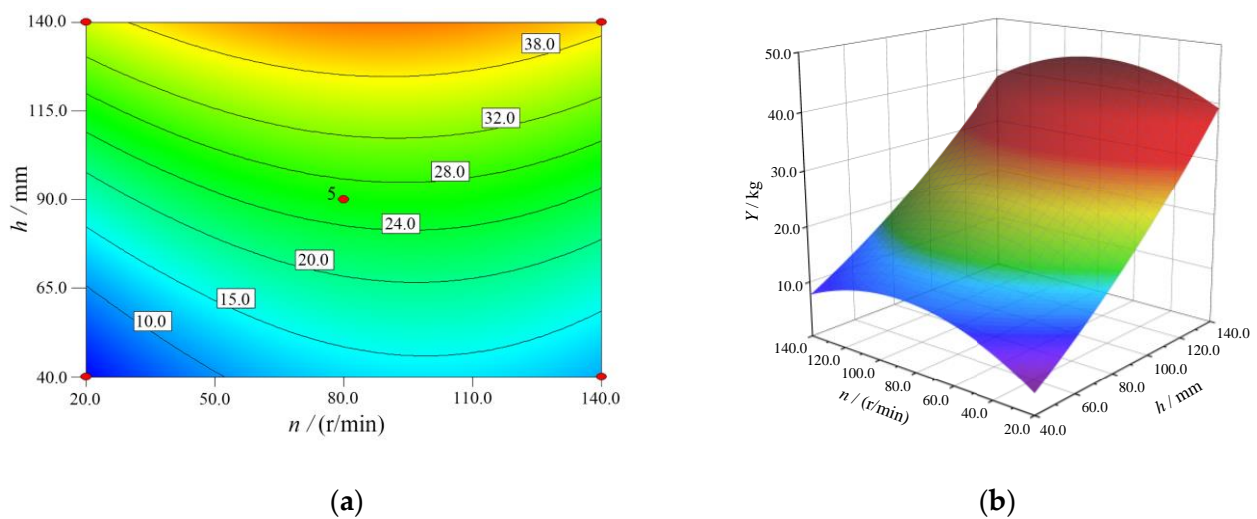


Figure 8. Influence of the forward speed and working depth on the soil-hilling quantity. (a) Contour map; (b) response surface diagram.

In conclusion, the order of significance in terms of the impact on the soil-hilling quantity Y is as follows: working depth h , rotation speed n , forward speed v_0 .

3.3. Parameter Optimization and Verification

3.3.1. Parameter Optimization

To obtain the combination of optimal parameters of the tooth roller device, we used the optimization module of Design-Expert V8.0.6.1 software [23,24]. The constraint conditions of the test factors and test indexes were:

$$\begin{cases} Y_{\min} = F(A, B, C) \\ s.t \begin{cases} A \in [4.0, 5.0] \\ B \in [40.0, 60.0] \\ C \in [80.0, 120.0] \end{cases} \end{cases} \quad (11)$$

The advancement results showed that the combination with the highest satisfaction degree was selected as the optimal combination of parameters: the forward speed v_0 is 4.5 km/h, the rotation speed n is 43.2 r/min, the working depth h is 100.0 mm, and the predicted value of the soil-hilling quantity $Y = 23.1$ kg.

3.3.2. Field Verification Test

Figure 9 was the field test process. A field performance test of the prototype was carried out referring to the methods specified in the Agricultural Machinery Promotion and Appraisal Outline of the Ministry of Agriculture and Rural Affairs of the People’s Republic of China, DG/T 149-2021 “film collector”. The parameter combination of the forward speed of the machine, the rotation speed of the nail-tooth roller, and the working depth were 4.5 km/h, 43.2 r/min, and 100.0 mm, respectively. The working width of the machine was 1600 mm. All of the above tests were repeated five times, and the results were calculated as an arithmetic average, as displayed in Table 5.



(a)



(b)

Figure 9. Residual film recovery machine test. (a) The test process; (b) the test results.

Table 5. Measurement results of the field test.

Items	Soil-Hilling Quantity					Residual Films Collection Rate	
	MAX/kg	MIN/kg	AVG/kg	C.V/%	PPV/kg	RE/%	AVG/%
Value	24.8	23.3	24.2	2.3	23.1	4.8	66.8

It can be seen from Table 5 that the soil-hilling quantity of the field test is 24.2 kg, the relative error is 4.8% compared with the predicted value, and the coefficient of variation

of the five experimental results is $2.3\% < 15\%$. The average residual films collection rate is 66.8%. The results show that the field test results are dependable, and the established EDEM simulation model could be used to predict the operation of the tooth roller device in the working process.

3.4. Discussion

The results show that the EDEM simulation model established in this paper can be used to predict the operation performance of the tooth roller device in the working process, and the research can provide important theoretical and methodological support for the design and parameter optimization of agricultural machinery equipment, which is consistent with the research results of Liu [25], Pan [26], Jia [27], and Hu et al. [28]. In addition, Luo et al. [29] designed a chaining screen tillage residual film recovery machine, and the test results showed that the residual film recovery rate was 85.07%. Our research group [30] designed a nail-toothed roller residual film recovery device in the early stage, and the residual film recovery rate was 70.56%, higher than the residual film recovery rate in this study. Guo et al. [31] designed a residual film recovery machine for the plough layer, and the field test results showed that the residual film recovery rate was 55.04%, which was lower than that in this study. A comprehensive analysis of the reason is that all types of residual film recovery machine are in the stage of research and development, and the structure of the key operating components is the main reason for the different residual film recovery rates. At the same time, in the field tests of the prototype, the research group [32] found that the area of residual film debris, soil type, soil moisture content, and region could all affect the operational effect of the residual film recovery machine.

4. Conclusions

In this paper, given the working qualities of the residual film recovery machine, the theoretical analysis method was used to determine the range of key operating parameters of the tooth roller device. Then, EDEM 2020 software was used to set up the physical model of a virtual simulation experiment. The Box–Behnken test technique of the Design-Expert V8.0.6.1 software was used to establish the quadratic regression model with the soil-hilling quantity Y as the test index, taking the forward speed v_0 , the rotation speed n , and the working depth h as the test factors. Furthermore, the order of significant factors that influence the test indexes was determined, and the optimal working parameters of the device were obtained as follows: the forward speed $v_0 = 4.5$ km/h, the rotation speed $n = 43.2$ r/min, the working depth $h = 100.0$ mm, and the soil-hilling quantity $Y = 23.1$ kg. Finally, field tests of the prototype were carried out using the best parameter combination. The results showed that the average collection rate of residual films is 66.8%, the soil-hilling quantity Y is 24.2 kg, and the relative error is 4.8%. This indicates that the EDEM simulation model we established can be used to predict the operational performance of the tooth roller device in the working process, and the optimal combination of working parameters can be used as the basis for the actual operation of the residual film recovery machine.

Author Contributions: Conceptualization, methodology, data curation, formal analysis, writing—original draft, writing—review and editing, Z.Z. and J.L.; investigation, X.W.; data curation, Y.Z.; funding acquisition, J.L. and X.W.; validation, S.X.; supervision, Z.S. All authors have read and agreed to the published version of the manuscript.

Funding: This research was funded by the National Natural Science Foundation of China (52175240; 51765057) and the Autonomous Region Postgraduate Research Innovation Project of Shihezi University in 2022 (XJ2022G011).

Institutional Review Board Statement: Not applicable.

Informed Consent Statement: Not applicable.

Data Availability Statement: All data are presented in this article in the form of figures and tables.

Conflicts of Interest: The authors declare that they have no conflict of interest or financial conflicts to disclose. This article does not contain any studies with human or animal subjects performed by any of the authors.

References

1. Chen, X.; Zhang, J.; Li, J.; Li, C.; Yang, Y. Design and Finite Element Analysis of Film Pick-up Components of Nail Tooth Drum Residual Film Recovery Device. *J. Agric. Mech. Res.* **2021**, *43*, 26–32.
2. Zhang, H.; Chen, X.; Yan, L.; Yang, S. Design and test of master-slave straw returning and residual film recycling combine machine. *Trans. Chin. Soc. Agric. Eng.* **2019**, *35*, 11–19.
3. Zhao, Y.; Chen, X.; Wen, H.; Zheng, X.; Niu, Q.; Kang, J. Research status and prospect of control technology for residual plastic film pollution in farmland. *Trans. Chin. Soc. Agric. Mach.* **2017**, *48*, 1–14.
4. Xue, S.; Chen, X.; Li, J.; Wang, X.; Zhang, Z. Design of and Experiment on a Film Removal Device of an Arc-Toothed Residual Film Recovery Machine before Sowing. *Appl. Sci.* **2021**, *11*, 8551. [[CrossRef](#)]
5. Liang, R.; Chen, X.; Zhang, B.; Meng, H.; Jiang, P.; Peng, X.; Kan, Z.; Li, W. Problems and countermeasures of recycling methods and resource reuse of residual film in cotton fields of Xinjiang. *Trans. Chin. Soc. Agric. Eng.* **2019**, *35*, 1–13.
6. You, J.; Zhang, B.; Wen, H.; Kang, J.; Song, Y.; Chen, X. Design and test optimization on spade and tine combined residual plastic film device. *Trans. Chin. Soc. Agric. Mach.* **2017**, *48*, 1–9.
7. He, Y.; Wu, M.; Xiang, W.; Yan, B.; Wang, J.; Bao, P. Application Progress of Discrete Element Method in Agricultural Engineering. *Chin. Agric. Sci. Bull.* **2017**, *33*, 133–137.
8. Zhang, H.; Yan, L.; Chen, X.; Jiang, D.; Yang, S. Simulation and test of film surface cleaning roller of residual film collector. *Int. Agric. Eng. J.* **2019**, *28*, 257–267.
9. Jiang, D.; Chen, X.; Yan, L.; Mo, Y.; Yang, S. Design and Experiment on Spiral Impurity Cleaning Device for Profile Modeling Residual Plastic Film Collector. *Trans. Chin. Soc. Agric. Mach.* **2019**, *50*, 137–145.
10. Wang, X.; Li, P.; He, J.; Wei, W.; Huang, Y. Discrete element simulations and experiments of soil-winged subsoiler interaction. *Int. J. Agric. Biol. Eng.* **2021**, *14*, 50–62. [[CrossRef](#)]
11. Tong, J.; Jiang, X.; Wang, Y.; Ma, Y.; Li, J.; Sun, J. Tillage force and disturbance characteristics of different geometric-shaped subsoilers via DEM. *Adv. Manuf.* **2020**, *8*, 392–404. [[CrossRef](#)]
12. Hang, C.; Huang, Y.; Zhu, R. Analysis of the movement behavior of soil between subsoilers based on the discrete element method. *J. Terramech.* **2017**, *74*, 35–43. [[CrossRef](#)]
13. Dai, F.; Guo, W.; Song, X.; Shi, R.; Zhao, W.; Zhang, F. Design and test of crosswise belt type whole plastic-film ridging-residual corn seeder on double ridges. *Int. J. Agric. Biol. Eng.* **2019**, *12*, 88–96.
14. Bernacki, H.; Haman, J.; Kanafojski, C. *Agriculture Machines, Theory and Construction*; China Machine Press: Beijing, China, 1985; Volume 1, pp. 171–195.
15. Hu, C.; Wang, X.; Chen, X.; Tang, X.; Zhao, Y.; Yan, C. Current situation and control strategies of residual film pollution in Xinjiang. *Trans. Chin. Soc. Agric. Eng.* **2019**, *35*, 223–234.
16. He, H.; Wang, Z.; Guo, L.; Zheng, X.; Zhang, J.; Li, W.; Fan, B. Distribution characteristics of residual film over a cotton field under long-term film residual and drip irrigation in an oasis agroecosystem. *Soil Tillage Res.* **2018**, *180*, 194–203. [[CrossRef](#)]
17. Liang, R.; Chen, X.; Jiang, P.; Zhang, B.; Meng, H.; Peng, X.; Kan, Z. Calibration of the simulation parameters of the particulate materials in film mixed materials. *Int. J. Agric. Biol. Eng.* **2020**, *13*, 29–36. [[CrossRef](#)]
18. Wang, X.; Hu, H.; Wang, Q.; Li, H.; He, J.; Chen, W. Calibration Method of Soil Contact Characteristic Parameters Based on DEM Theory. *Trans. Chin. Soc. Agric. Mach.* **2017**, *48*, 78–85.
19. Dai, F.; Song, X.; Zhao, W.; Zhang, F.; Ma, H.; Ma, M. Simulative Calibration on Contact Parameters of Discrete Elements for Covering Soil on Whole Plastic Film residual on Double Ridge. *Trans. Chin. Soc. Agric. Mach.* **2019**, *50*, 49–56, 77.
20. Ucgul, M.; Sannders, C.; Fielke, J. Discrete element modelling of top soil burial using a full scale mouldboard plough under field conditions. *Biosyst. Eng.* **2017**, *160*, 140–153. [[CrossRef](#)]
21. Zhao, S.; Wang, J.; Chen, J.; Yang, Y.; Tan, H. Design and Experiment of Fitting Curve Subsoiler of Conservation Tillage. *Trans. Chin. Soc. Agric. Mach.* **2018**, *49*, 82–92.
22. Yang, Y.; Wen, B.; Ding, L.; Li, L.; Chen, X.; Li, J. Soil particle modeling and parameter calibration for use with discrete element method. *Trans. ASABE* **2021**, *64*, 2011–2023. [[CrossRef](#)]
23. Ge, Y.; Zhang, L.; Gu, J.; Fu, W.; Zhu, R.; Zhang, H. Parameter optimization and experiment of dual roller harvesting device for safflower. *Trans. Chin. Soc. Agric. Eng.* **2015**, *31*, 35–42.
24. Shi, G.; Li, J.; Kan, Z.; Ding, L.; Ding, H.; Zhou, L.; Wang, L. Design and Parameters Optimization of a Provoke-Suction Type Harvester for Ground Jujube Fruit. *Agriculture* **2022**, *12*, 409. [[CrossRef](#)]
25. Liu, L.; Ma, C.; Liu, Z. EDEM-based Parameter Optimization and Experiment of Full-layer Fertilization Shovel for Strip Subsoiling. *Trans. Chin. Soc. Agric. Mach.* **2021**, *52*, 74–83.

26. Pan, J.; Chen, F.; Hu, J.; Yue, R.; Yao, M.; Li, J. Simulation and Optimization Design of Finger-clamping Seedling Picking Claw Based on EDEM-RecurDyn. *Trans. Chin. Soc. Agric. Mach.* **2022**. Available online: <https://kns.cnki.net/kcms/detail/11.1964.s.20220316.2211.008.html> (accessed on 26 March 2022).
27. Jia, L.; Jiang, Y.; Sun, J.; Fu, T.; Jiang, L.; Wang, J. EDEM-based simulation and test of disc blade rollers of disc spring tooth combination type paddy grader. *Acta Agric. Univ. Jiangxiensis* **2021**, *43*, 1406–1414.
28. Hu, T.; Hu, J.; Bi, Y.; Yang, M.; Li, M.; Yang, J. Design of Sea-buckthorn roller screen based on EDEM numerical. *J. Chin. Agric. Mech.* **2021**, *42*, 122–129.
29. Luo, K.; Yuan, P.; Jin, W.; Yan, J.; Bai, S.; Zhang, C.; Zhang, X. Design of chain-sieve type residual film recovery machine in plough layer and optimization of its working parameters. *Trans. Chin. Soc. Agric. Eng.* **2018**, *34*, 19–27.
30. Chen, X.; Chen, X.; Li, J.; Li, C.; Yang, Y. Design and test of nail-teeth roller-type residual film recovery device before sowing. *Trans. Chin. Soc. Agric. Eng.* **2020**, *36*, 30–39.
31. Guo, W.; He, X.; Wang, L.; Zhao, P.; Hu, C.; Hou, S.; Wang, X. Development of a comb tooth loosening and pneumatic stripping plough layer residual film recovery machine. *Trans. Chin. Soc. Agric. Eng.* **2020**, *36*, 1–10.
32. Wang, X.; Zhang, Z.; Zhao, Y.; Xue, S.; Li, J. Design and test of arc-shaped film binding nail teeth. *J. Chin. Agric. Mech.* **2021**, *42*, 24–29.